Solar hydrogen-producing bionanodevice outperforms natural photosynthesis

Carolyn E. Lubner[a], Amanda M. Applegate[a], Philipp Knörzer[b], Alexander Ganago[c,1], Donald A. Bryant[c,d], Thomas Happe[b], and John H. Golbeck[a,c,2]

[a]Department of Chemistry, The Pennsylvania State University, University Park, PA 16802; [b]Ruhr-Universität Bochum, Lehrstuhl für Biochemie der Pflanzen, AG Photobiotechnologie, 44780 Bochum, Germany; [c]Department of Biochemistry and Molecular Biology, The Pennsylvania State University, University Park, PA 16802; and [d]Department of Chemistry and Biochemistry, Montana State University, Bozeman, MT 59717

Edited by* David Baker, University of Washington, Seattle, WA, and approved November 2, 2011 (received for review September 6, 2011)

Although a number of solar biohydrogen systems employing photosystem I (PSI) have been developed, few attain the electron transfer throughput of oxygenic photosynthesis. We have optimized a biological/organic nanoconstruct that directly tethers F_B, the terminal [4Fe-4S] cluster of PSI from *Synechococcus* sp. PCC 7002, to the distal [4Fe-4S] cluster of the [FeFe]-hydrogenase (H_2ase) from *Clostridium acetobutylicum*. On illumination, the PSI–[FeFe]-H_2ase nanoconstruct evolves H_2 at a rate of $2{,}200 \pm 460$ μmol mg chlorophyll^{-1} h^{-1}, which is equivalent to 105 ± 22 e$^-$PSI^{-1} s^{-1}. Cyanobacteria evolve O_2 at a rate of approximately 400 μmol mg chlorophyll^{-1} h^{-1}, which is equivalent to 47 e$^-$PSI^{-1} s^{-1}, given a PSI to photosystem II ratio of 1.8. The greater than twofold electron throughput by this hybrid biological/organic nanoconstruct over in vivo oxygenic photosynthesis validates the concept of tethering proteins through their redox cofactors to overcome diffusion-based rate limitations on electron transfer.

biohybrid | solar fuels | light harvesting | green biophysics | renewable energy

In oxygenic photosynthesis, the overall reaction $H_2O + 2$ ferredoxin$_{ox} + 4\ h\nu \rightarrow 1/2\ O_2 + 2H^+ + 2$ ferredoxin$_{red}$ is carried out in two separate photochemical half-reactions. Photosystem II (PSII) catalyzes the anodic half-cell reaction $H_2O +$ plastoquinone-9 $+ 2\ h\nu \rightarrow 1/2\ O_2 +$ plastoquinol-9, while photosystem I (PSI) catalyzes the cathodic half-cell reaction cytochrome $c_{6(red)}$ + ferredoxin$_{ox}$ + 1 $h\nu \rightarrow$ cytochrome $c_{6(ox)}$ + ferredoxin$_{red}$. Visible photons provide the energy necessary to drive these otherwise thermodynamically unfavorable half-cell reactions to completion (1). Cyanobacteria evolve O_2 at a rate of approximately 400 μmol mg Chl^{-1} h^{-1} (2, 3) in a process limited by diffusion-governed electron transfer steps (Fig. 1*A*), in particular the slow interaction of plastoquinol-9 with the cytochrome b_6f complex (4). Once electrons leave PSI, diffusionally governed electron transfer steps constrain the rate of interaction of ferredoxin with other enzymes, including ferredoxin:NADP$^+$ oxidoreductase. Were it possible to directly connect redox proteins through their redox centers, electrons could be vectored preferentially thereby eliminating any dependence on diffusional electron transfer (5, 6, 7). Here we report that by engineering a nanoconstruct in which both the electron donor (cytochrome c_6) and acceptor (here: [FeFe]-H_2ase) are tethered to PSI in vitro, rate-limiting, diffusion-based electron transfer reactions are eliminated (Fig. 1*B*), resulting in electron transfer rates that exceed those of natural photosynthesis.

The approach connects PSI to an [FeFe]-H_2ase (8) using a molecular wire, which separates the [4Fe-4S] clusters of each enzyme by a defined distance (5). By introducing an exchangeable sulfhydryl ligand to the most solvent-exposed iron atom of PSI, the molecular wire can be attached by a ligand exchange mechanism. This is achieved by site-specific conversion of a ligating Cys residue (C13) of F_B, the terminal [4Fe-4S] cluster, to a Gly (9–11) and by chemically rescuing the cluster with a small sulfhydryl-containing molecule (11). Because [FeFe]-H_2ases also contain [4Fe-4S] clusters, which constitute an electron transfer pathway between the surface of the enzyme and its catalytic site (12, 13), a similar strategy is used to introduce an exchangeable ligand at the distal [4Fe-4S] cluster (C97G). A tether that contains two sulfhydryl groups serves as a chemical rescue agent for both the F_B cluster of PSI and the distal [4Fe-4S] cluster of [FeFe]-H_2ase, thereby providing a pathway for electrons to quantum mechanically tunnel between the two proteins.

Results and Discussion

When variant PSI complexes (PSI_{C13G}) are tethered to the variant H_2ase protein ([FeFe]-H_2ase$_{C97G}$) using 1,6-hexanedithiol and assayed in 50 mM Tris buffer at pH 8.3, the light-induced H_2 evolution rate was 30.3 μmol H_2 mg Chl^{-1} h^{-1} (5). To ameliorate the issue of donor side rate limitation, cytochrome c_6 (Cyt c_6) was chemically cross-linked to PSI_{C13G} using a zero-length cross-linking agent. When the Cyt c_6-cross-linked PSI_{C13G} complex was tethered to [FeFe]-H_2ase$_{C97G}$ using 1,6-hexanedithiol and assayed in 50 mM Tris buffer at pH 8.3, the light-induced H_2 evolution rate increased approximately sevenfold to 200 μmol H_2 mg Chl^{-1} h^{-1}.

Light-induced H_2 production was assayed using a variety of wire lengths, buffers, and pH values (Table 1). Molecular wires containing 3–10 methylene groups or one or two phenyl groups were all found to support high rates of light-driven H_2 evolution, typically between 160 and 330 μmol H_2 mg Chl^{-1} h^{-1}. All molecular wire lengths were sufficiently short (6–15 Å) so that electron transfer would outcompete the backreaction between the F_B cluster and the primary donor, P_{700}. When Tris buffer was replaced with Tricine buffer, the rate increased 6.6-fold from 200 to 1,340 μmol H_2 mg Chl^{-1} h^{-1} in Cyt c_6-cross-linked PSI_{C13G} complexes containing 1,6-hexanedithiol as the molecular wire. Tris buffer has been shown to negatively impact biological samples; it is known to interfere with the manganese cluster of PSII and is an inhibitor of several dehydrogenases (14). The highest rates were achieved with a cross-linked Cyt c_6–PSI_{C13G}–[FeFe]-H_2ase$_{C97G}$ nanoconstruct using 1,8-octanedithiol in a medium of Na-phosphate buffer at pH 6.5. A one-time maximal rate of light-induced H_2 evolution of 2,830 μmol mg Chl^{-1} h^{-1} was observed, with an average rate of light-induced H_2 evolution of $2{,}200 \pm 460$ μmol mg Chl^{-1} h^{-1}. Octanedithiol may be optimal simply because it provides sufficient length to avoid steric hindrance between the two proteins. Use of a conjugated wire would, in principle, allow for faster electron transfer, and hence, for

Author contributions: C.E.L., D.A.B., and J.H.G. designed research; C.E.L., A.M.A., P.K., and A.G. performed research; C.E.L., A.M.A., and J.H.G. analyzed data; and C.E.L., A.M.A., D.A.B., T.H., and J.H.G. wrote the paper.

The authors declare no conflict of interest.

*This Direct Submission article had a prearranged editor.

[1]Present address: EECS Department, University of Michigan, 1301 Beal Avenue, Ann Arbor, MI 48109.

[2]To whom correspondence should be addressed. E-mail: jhg5@psu.edu.

This article contains supporting information online at www.pnas.org/lookup/suppl/doi:10.1073/pnas.1114660108/-/DCSupplemental.

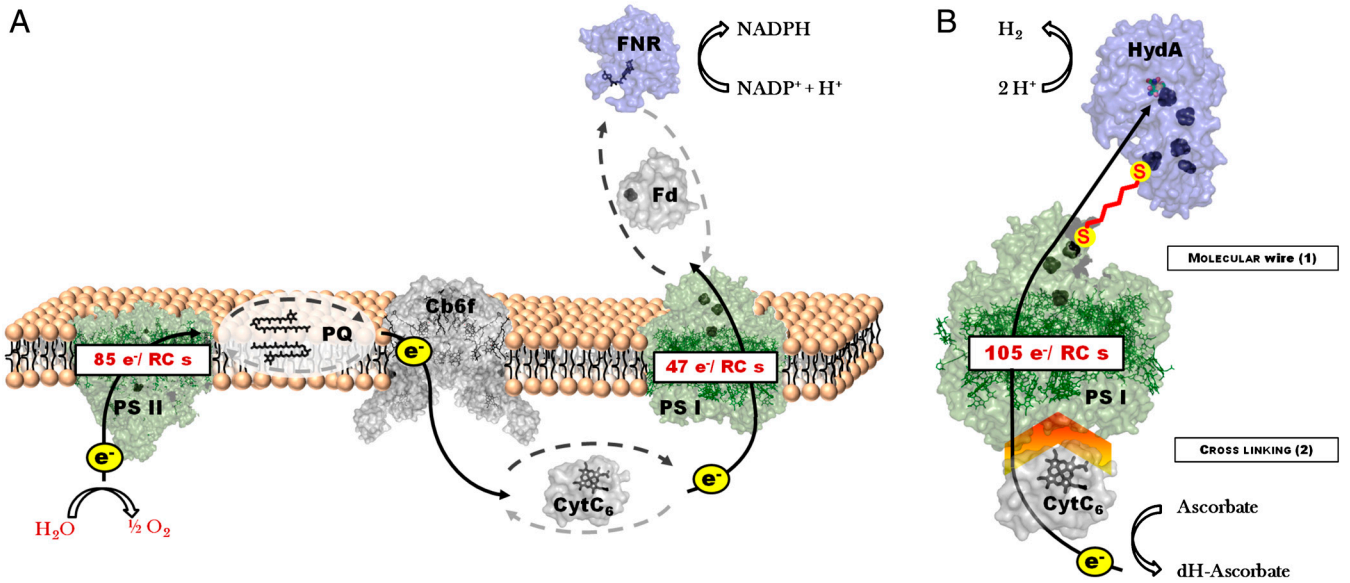

Fig. 1. Schematic comparison of electron flow in (*A*) in vivo photosynthesis and (*B*) the photosynthetic nanoconstructs described here. Rates given indicate the electron throughput through each of the photosynthetic reaction centers in each scenario. Electron transfer is primarily diffusionally governed in *A* and through bonds in *B*. Direct electron transfer reactions are indicated as black solid arrows, diffusion-based steps as black dashed arrows. Protein complexes are shown as crystal structures. Cross-linking in *B* is indicated as a red arrow. The molecular wire structure is shown in red. (Cyt c_6: cytochrome c_6, Cb_6f: cytochrome b_6f complex, Fd: ferredoxin, FNR: ferredoxin:$NADP^+$ oxido reductase, HydA: hydrogenase, PQ: plastoquinone pool).

longer distances; however, this is not a constraint in the current construct. Rather, the value of a longer conjugated wire may lie in extracting the electron from a cofactor more distant from the protein surface, for example, at the quinone site.

In any given sample, H_2 was evolved continuously over the course of 4 h, with an ultimate decline in rate due to the depletion of the sacrificial donor, sodium ascorbate. Upon addition of fresh ascorbate, light-induced H_2 evolution resumed at the initially measured rate. Full recovery of H_2-evolving ability was observed to occur over the course of 100 d when the sample was stored at room temperature under anoxic conditions.

All control experiments were negative: i.e., there was no measurable light-driven H_2 evolution when the Cyt c_6-cross-linked PSI_{C13G} complexes and the [FeFe]-H_2ase_{C97G} variant were combined in the absence of a dithiol molecular wire or when wild-type PSI or wild-type [FeFe]-H_2ase were substituted for their respective Cys-to-Gly variants. Additionally, in the absence of an electron donor or illumination or employing a wire that is unable to tether both proteins (i.e., 1-hexanethiol), no hydrogen was evolved.

The average rate of light-induced hydrogen production from this study ($2{,}200 \pm 460$ μmol mg Chl^{-1} h^{-1}) can be compared with the rate of electron transfer through PSI in cyanobacteria. Under high light and in the presence of high concentrations of bicarbonate, the contribution of the cyclic electron transfer around PSI in the cyanobacterium *Synechococcus* sp. PCC 7002 is negligible, as it accounts for only 2.5% of the total electron transfer through PSI (15). Under these conditions, the rate of O_2 evolution is in the range of 410 ± 25 μmol O_2 mg Chl^{-1} h^{-1} (2, 3). Because four electrons must be removed from two H_2O molecules to evolve one molecule of O_2, this corresponds to an overall electron transfer rate of $1{,}640 \pm 100$ μmol e^- mg Chl^{-1} h^{-1}.

To determine the electron transfer rate individually through PSI and PSII, the mismatch in the ratio of PSI to PSII in whole cells as well as the difference in the respective reaction center chlorophyll compositions must be taken into account. The ratio of PSI to PSII in *Synechococcus* sp. PCC 7002 grown to the end of exponential phase has been measured to be 1.8 (2, 3). On the average, if N electrons are transferred through each PSII per second, then each PSI transfers $N/1.8$ electrons per second. In cyanobacteria, each PSII complex is associated with roughly 35 molecules of Chl (16), while each PSI is associated with 96 Chl molecules (17). Therefore, the total number of Chl molecules in the cell associated with PSI is about five times larger than the total number of Chl molecules associated with PSII. (The very large optical cross-section of PSII, due to the presence of phycobilisomes, is a major reason why the two photosystems are not equimolar in cyanobacteria.) Because of the inequality in the amount of chlorophyll associated with each reaction center, it is more relevant to compare and contrast photosynthetic electron

Table 1. Effect of buffer and pH on hydrogen production and electron throughput

pH	Buffer (50 mM)	Molecular wire	Rate of H_2 production (μmol H_2 mg Chl^{-1} h^{-1})	Electron throughput (e^- PSI^{-1} s^{-1})
8.3	Tris·HCl	1,6-hexanedithiol	200 ± 120	10 ± 6
	Tricine	1,6-hexanedithiol	1,340 ± 420	64 ± 20
7.0	Sodium phosphate	1,6-hexanedithiol	1,360 ± 20	65 ± 1
6.5	Pipes	1,6-hexanedithiol	1,130 ± 200	54 ± 10
	Sodium phosphate	1,6-hexanedithiol	1,540 ± 150	73 ± 7
	Sodium phosphate	1,8-octanedithiol	2,200 ± 460	105 ± 22
	Sodium phosphate	1,10-decanedithiol	1,200 ± 80	57 ± 4
6.0	Sodium phosphate	1,6-hexanedithiol	1,430 ± 170	68 ± 8

H_2 evolution rates for Cyt c_6 cross-linked-PSI_{C13G}–[FeFe]-H_2ase_{C97G} nanoconstructs as a function of buffer and pH. H_2 production rates as a function of aliphatic molecular wires are shown for the optimal buffer and pH conditions. All conditions explored led to high rates of light-induced hydrogen production. Rates shown are the average of at least three independent replicates. Standard deviations are given.

transport rates when expressed in units of electrons per reaction center (RC) per second. Taking these units into account, we obtain that, on the average each PSI transfers 47 e^- RC_{PSI}^{-1} s^{-1}, while each PSII transfers 85 e^- RC_{PSII}^{-1} s^{-1} (*SI Text*). Electron transfer in these cells may be operating near the kinetic limit imposed by the rate-limiting interaction of plastoquinone with the cytochrome b_6f complex (4).

Electron throughput is considerably faster in isolated PSI complexes, although extremely high concentrations of Cyt c_6 and flavodoxin are required to maintain these rates (Table 2). In the presence of 180 μM Fld, 80 μM (noncross-linked) Cyt c_6, and PSI at 5 μg mL^{-1} Chl, Fld is reduced at a rate of $9{,}440 \pm 440$ μmol mg Chl^{-1} h^{-1}, which is equivalent to 230 ± 11 e^- RC_{PSI}^{-1} s^{-1}. Thus, isolated PSI complexes are capable of an electron transfer throughput at least five times higher than the average rates that occur in vivo (2, 3). These high rates may be useful under high light conditions particularly when cyclic electron transfer is required to produce additional ATP. Note, however, that the maximal measured electron transfer rate in isolated PSI complexes was only achieved using a nonphysiological molar excess of Fld (3,000-fold) and Cyt c_6 (1,430-fold) over PSI.

In contrast, the nanodevice constructed here is comprised of cross-linked Cyt c_6, PSI, a molecular wire, and an [FeFe]-H_2ase. The electron transfer throughput in the corresponding nanoconstruct was 4,400 μmol mg Chl^{-1} h^{-1}, which is equivalent to 105 e^- RC_{PSI}^{-1} s^{-1}. Thus, electron flow is more than two times higher than the calculated electron transfer rates in PSI during in vivo photosynthesis in *Synechococcus* sp. PCC 7002. Because Cyt c_6 is cross-linked to PSI, its concentration is three orders of magnitude lower than used for the studies that employ soluble Cyt c_6, i.e., 0.066 μM vs. 80 μM Cyt c_6. Moreover, by optimizing parameters, a long-lived photocatalytic system was achieved that evolved H_2 at a rate nearly two orders of magnitude (a 70-fold increase) higher than other comparable systems (5, 18). By eliminating diffusion-limiting processes in the nanoconstructs, the electron throughput of PSI is greatly increased compared to that in vivo.

Nevertheless, there are still several factors that may limit the rate of light-induced H_2 evolution. These include an unknown efficiency of Cyt c_6 cross-linking as well as an unknown coupling efficiency of H_2ase with the PSI-wire assembly. The presence of unproductive species resulting from PSI–PSI or H_2ase-H_2ase homodimers is similarly unknown. There also may be a limitation due to electron transfer from the sacrificial electron donor, ascorbate, to Cyt c_6 that might be overcome by placing the nanoconstruct assembly on an electrode. Lastly, the light intensity was approximately 45% of saturation based on studies with wild-type PSI using flavodoxin as an electron acceptor.

In conclusion, the electron transfer throughput of the Cyt c_6–PSI_{C13G}-molecular wire-[FeFe]-H_2ase_{C97G} nanoconstruct was shown to surpass that of oxygenic photosynthesis, thereby validating the concept of using molecular wires to overcome limitations of diffusion-based electron transfer reactions. The modular design and highly flexible nature of these hybrid nanoconstructs, along with their stability, should allow for their incorporation into a variety of solar biofuel producing systems.

Table 2. Dependency of electron throughput rates in PSI on soluble redox partners

Cyt c_6	Fld	Rate of Fld reduction (μmol Fld mg Chl^{-1} h^{-1})	Electron throughput (e^- PSI^{-1} s^{-1})
0 μM*	45 μM	80 ± 4	2 ± 0.1
0 μM†	45 μM	1,720 ± 50	40 ± 1
20 μM	45 μM	4,240 ± 140	100 ± 3
40 μM	90 μM	7,280 ± 240	170 ± 6
80 μM	180 μM	9,440 ± 440	230 ± 11

Rates of Fld reduction in isolated PSI complexes as a function of soluble Cyt c_6 and Fld concentration. Rates shown are the average of at least three independent replicates. Standard deviations are given.
*40 μM 1,6-dichlorophenolindophenol (DCPIP).
†220 μM phenazine methosulfate (PMS).

Materials and Methods

Purification of PSI, Cyt c_6 and [FeFe]-H_2ase. PSI was purified from *Synechococcus* sp. PCC 7002 (19) and the C13G/C33S variant of PsaC from *Synechococcus* sp. PCC 7002 was overproduced in *Escherichia coli*, purified, reconstituted, and stored under strictly anoxic conditions (11). Recombinant PsaD from *Synechococcus* sp. PCC 7002 (20) and Cyt c_6 from *Synechocystis* sp. PCC 6803 (21) were overproduced in *E. coli* and purified as described. Wild-type and C97G variant *C. acetobutylicum* [FeFe]-H_2ase was produced as described (5).

Rebuilding PSI from P_{700}/F_X Cores and Recombinant PsaC, PsaD, and Cytochrome c_6. PSI was reconstituted from P_{700}/F_X cores (22) and recombinant C13G/C33G PsaC and PsaD at a ratio of 1:20:10 under anoxic conditions. Excess unbound C13G/C33G PsaC and PsaD were removed by ultrafiltration (100-kDa cutoff membrane) under anoxic conditions. Time-resolved optical spectroscopy was used to confirm the rebinding of PsaC and PsaD to the P_{700}/F_X cores, as evidenced by the reappearance of an approximately 65 ms kinetic phase associated with the backreaction from reduced F_A/F_B [4Fe-4S] clusters and P_{700} (23). These PSI complexes will hereafter be described as "reconstituted PSI." Cyt c_6 was cross-linked to reconstituted PSI (see above) using the zero-length cross-linking agent 1-ethyl-3-[3-dimethylaminopropyl]carbodiimide and *N*-hydroxysulfosuccinimide following the manufacturer's protocol (Thermo Scientific) (24, 25).

Time-Resolved Optical Spectroscopy. Transient absorbance changes at 820 nm were measured to determine the electron transfer properties of reconstituted PSI and wild-type PSI complexes to which Cyt c_6 had been cross-linked. Transient absorbance changes were measured at room temperature with a laboratory built, dual beam spectrometer as described (26). The sample was contained in a 10 × 2 mm quartz cuvette and was positioned so the optical path length was 10 mm. The measuring and reference beam intensities were balanced using a variable density, optical filter wheel. The difference signal was amplified with an 11A33 differential comparator and displayed on a DSA610 digital signal analyzer (Tektronix). The sample contained reconstituted PSI at a concentration of 50 μg Chl mL^{-1} in 50 mM Tris·HCl pH 8.3, 10 mM NaCl, 10 mM $MgCl_2$, 10 μM 1,6-dichlorophenolindophenol, 10 mM sodium ascorbate, and 0.05% (vol./vol.) Triton X-100.

Steady-State Kinetic Measurements. The rate of flavodoxin photoreduction was measured in a 700 μL volume (10 × 2 mm quartz cuvette) with the same sample composition as for the time-resolved optical studies, except for 5 μg Chl mL^{-1}, 2.5 mM ascorbate, and the addition of varying amounts of flavodoxin (45–180 μM) and Cyt c_6 (0–80 μM) as specified in Table 2. Recombinant flavodoxin from *Synechococcus* sp. PCC 7002 was produced and purified as described (27). Flavodoxin reduction was measured by the change in the absorption at 580 nm and by using the molar extinction coefficient 4.25 L $mmol^{-1}$.

Construction of PSI-Molecular Wire Nanoconstructs. PSI-molecular wire-[FeFe]-H_2ase nanoconstructs were assayed for light-induced H_2 generation by using the reconstituted PSI proteins to which Cyt c_6 had been cross-linked. The nanoconstruct samples were assembled overnight in a sealed vial in the dark under anoxic conditions such that each contained 13.4 μg Chl mL^{-1}, 0.30 μM [FeFe]-H_2ase, and 200 nM molecular wire for samples with a total volume of 0.500 mL. Samples with a final volume of 0.250 mL contained 5.696 μg Chl mL^{-1}. Unless otherwise noted, samples were buffered with 50 mM Tris·HCl, pH 8.3, containing 10 mM $MgCl_2$, and 10 mM NaCl.

Evaluation and Optimization of H_2 Production. Assembled PSI-molecular wire-[FeFe]-H_2ase nanoconstructs were purged with argon in the dark prior to testing to remove any residual H_2. Prior to illumination, anoxic solutions of sodium ascorbate (100 mM) and phenazine methosulfate (PMS) (30 μM) were added to the sealed vials using a gas-tight syringe. The samples were illuminated continuously (5 mm path length) for 1–3 h using a 100 W xenon arc lamp (996 μmol photons m^{-2} s^{-1}). A clear polycarbonate culture flask filled with doubly distilled water was used to remove infrared radiation and maintain a constant sample temperature (20–22 °C). H_2 production for each PSI-molecular wire-[FeFe]-H_2ase nanoconstruct was evaluated using gas chromatography (GC) before and immediately after illumination by removing 200 μL of the headspace gas using an airtight locking syringe. GC analyses were performed with a Shimadzu GC-8A gas chromatograph equipped with

a ShinCarbon 80/100 column (2 m × 2 mm) and thermal conductivity detector (100 mA detector current) with ultrapure N_2 as the carrier gas (flow rate 0.75 mL min^{-1}).

Long-Term Assays. Long-term assays were conducted by intermittent testing of nanoconstruct samples (13.4 μg Chl mL^{-1}) prepared using 1,6-hexanedithiol, 1,4-benzenedithiol, or 4,4′-biphenyldithiol molecular wires buffered in 50 mM Tris·HCl, pH 8.3. Anoxic conditions were maintained between assays. Fresh anoxic stock solutions of the molecular wire (200 nM), sodium ascorbate (100 mM), and PMS (30 μM) were added to the samples before each assay.

ACKNOWLEDGMENTS. This work was funded by the US Department of Energy, Basic Energy Sciences, Division of Materials Sciences and Engineering, under Contract DE-FG-05-05-ER46222. Further financial support (T.H.) by the EU-SolarH2 program, the Bundesministrium für Bildung und Forschung (Bio-H2), and the Volkswagen foundation (LigH2t) is gratefully acknowledged.

1. Golbeck JH (1993) Shared thematic elements in photochemical reaction centers. *Proc Natl Acad Sci USA* 90:1642–1646.
2. Schluchter WM, Zhao JD, Bryant DA (1993) Isolation and characterization of the *ndhF* gene of *Synechococcus* sp. PCC 7002 and initial characterization of an interposon mutant. *J Bacteriol* 175:3343–3352.
3. Nomura CT, Persson S, Shen G, Inoue-Sakamoto K, Bryant DA (2006) Characterization of two cytochrome oxidase operons in the marine cyanobacterium *Synechococcus* sp. PCC 7002: Inactivation of *ctaDI* affects the PS I:PS II ratio. *Photosynth Res* 87:215–228.
4. Cramer WA (2004) Ironies in photosynthetic electron transport: A personal perspective. *Photosynth Res* 80:293–305.
5. Lubner CE, et al. (2010) Wiring an [FeFe]-hydrogenase with photosystem I for light-induced hydrogen production. *Biochemistry* 49(48):10264–10266.
6. Lubner CE, Grimme RA, Bryant DA, Golbeck JH (2010) Wiring photosystem I for direct solar hydrogen production. *Biochemistry* 49:404–414.
7. Lubner CE, Heinnickel M, Bryant DA, Golbeck JH (2011) Wiring photosystem I for electron transfer to a tethered redox dye. *Energy Environ Sci* 4:2428–2434.
8. Melis A, Happe T (2001) Hydrogen production green algae as a source of energy. *Plant Physiol* 127:740–748.
9. Mehari T, et al. (1995) Modified ligands to F_A and F_B in photosystem I. 1. Structural constraints for the formation of iron-sulfur clusters in free and rebound PsaC. *J Biol Chem* 270:28108–28117.
10. Jung YS, et al. (1996) Modified ligands to F_A and F_B in photosystem I- proposed chemical rescue of a [4Fe-4S] cluster with an external thiolate in alanine, glycine, and serine mutants of PsaC. *J Biol Chem* 271:31135–31144.
11. Antonkine ML, et al. (2007) Chemical rescue of a site-modified ligand to a [4Fe-4S] cluster in PsaC, a bacterial-like dicluster ferredoxin bound to photosystem I. *Biochim Biophys Acta* 1767:712–724.
12. Girbal L, et al. (2005) Homologous and heterologous overexpression in *Clostridium acetobutylicum* and characterization of purified clostridial and algal Fe-only hydrogenases with high specific activities. *Appl Environ Microbiol* 71:2777–2781.
13. Peters JW, Lanzilotta WN, Lemon BJ, Seefeldt LC (1998) X-ray crystal structure of the Fe-only hydrogenase CpI from *Clostridium pasteurianum* to 1.8 angstrom resolution. *Science* 282:1853–1858.
14. Perrin DD, Dempsey B (1974) *Buffers for pH and Metal Ion Control*, ed A Albert (Chapman & Hall, London, New York), pp 58–61.
15. Yu L, Zhao JD, Muhlenhoff U, Bryant DA, Golbeck JH (1993) PsaE is required for in vivo cyclic electron flow around Photosystem I in the cyanobacterium *Synechococcus* sp. PCC 7002. *Plant Physiol* 103:171–180.
16. Guskov A, et al. (2010) Recent progress in the crystallographic studies of Photosystem II. *Chem Phys Chem* 11:1160–1171.
17. Jordan P, et al. (2001) Three dimensional structure of Photosystem I at 2.5 Å resolution. *Nature* 411:909–917.
18. Iwuchukwu IJ, et al. (2009) Self-organized photosynthetic nanoparticle for cell-free hydrogen production. *Nat Nanotechnol* 5:73–79.
19. Li N, et al. (1991) Polypeptide composition of the photosystem I complex and the photosystem I core protein from *Synechococcus* sp. PCC 6301. *Biochim Biophys Acta* 1059:215–225.
20. Zhao J, Warren PV, Li N, Bryant DA, Golbeck JH (1990) Reconstitution of electron transport in photosystem I with PsaC and PsaD proteins expressed in *Escherichia coli*. *FEBS Lett* 276:175–180.
21. Diaz A, et al. (1994) Cloning and correct expression in *E. coli* of the *petJ* gene encoding cytochrome c_6 from *Synechocystis* 6803. *FEBS Lett* 347:173–177.
22. Parrett KG, Mehari T, Warren PG, Golbeck JH (1989) Purification and properties of the intact P_{700} and F_X-containing photosystem I core protein. *Biochim Biophys Acta* 973:324–332.
23. Golbeck JH, Mehari T, Parrett K, Ikegami I (1988) Reconstitution of the photosystem I complex from the P_{700} and F_X-containing reaction center core protein and the F_A/F_B polypeptide. *FEBS Lett* 240:9–14.
24. Grabarek Z, Gergely J (1990) Zero-length crosslinking procedure with the use of active esters. *Anal Biochem* 185:131–135.
25. Staros JV, Wright RW, Swingle DM (1986) Enhancement by N-hydroxysulfosuccinimide of water-soluble carbodiimide-mediated coupling reactions. *Anal Biochem* 156:220–222.
26. Vassiliev IR, Jung YS, Mamedov MD, Semenov AY, Golbeck JH (1997) Near-IR absorbance changes and electrogenic reactions in the microsecond-to-second time domain in Photosystem I. *Biophys J* 72:301–315.
27. Zhao J, Li R, Bryant DA (1998) Measurement of photosystem I activity with photoreduction of recombinant flavodoxin. *Anal Biochem* 264:263–270.